Structural, transport, and magnetic properties of pure and La-doped RuSr$_2$GdCu$_2$O$_8$

P. Mandal,[1,2] A. Hassen,[1] J. Hemberger,[1] A. Krimmel,[1] and A. Loidl[1]

[1]*Experimentalphysik V, Elektronische Korrelationen and Magnetismus, Insitut für Physik, Universität Augsburg,
D-86159 Augsburg, Germany*
[2]*Saha Insitut of Nuclear Physics, 1/AF Bidhannagar, Calcutta 7000064, India*

The structural properties, the electrical resistivity, and the magnetic properties of the "ferromagnetic" superconductor Ru(Sr$_{1-x}$La$_x$)$_2$GdCu$_2$O$_8$ are systematically investigated as a function of La doping, temperature, and external magnetic field. These compounds are characterized by superconductivity ($T_c = 45$ K) in the CuO$_2$ planes, coexisting with weak ferromagnetism in the RuO$_2$ planes. Pure Ru-1212 reveals properties similar to those observed in heavily underdoped high-T_c materials. We present a detailed investigation of the dc and ac magnetic properties. Doping with La gives no significant structural changes but reduces the charge-carrier density and already at $x = 0.03$ superconductivity is completely suppressed while the magnetic ordering temperatures are slightly enhanced. On increasing x the charge carriers are localized at low temperatures and for $x = 0.1$ semiconducting transport properties dominate below room temperature.

I. INTRODUCTION

After early reports[1] of superconductivity in $R_{1.4}$Ce$_{0.6}$RuSr$_2$Cu$_2$O$_{10-\delta}$ (R=Gd: T_c=42 K; R=Eu: T_c=32 K) coexisting with magnetism with high-ordering temperatures (R=Gd: T_N=180 K; R=Eu: T_N=122 K) a class of hybrid ruthenocuprates (Ru-1212) has been synthesized which shows coexistence of weak ferromagnetism with superconductivity.[2–7] These compounds can be derived from the 123 high-T_c superconductors by replacing the CuO chains by RuO$_2$ layers and are characterized by a sequence of CuO$_2$ double layers carrying the superconductivity and RuO$_2$ layers responsible for the weak ferromagnetism. RuSr$_2$GdCu$_2$O$_8$ shows magnetic order below 135 K and the onset of superconductivity at 45 K.[3] For the isostructural Eu compound these transition temperatures are shifted to 32 K and 132 K, respectively.[6,7] The intrinsic nature of bulk superconductivity and the uniform character of the magnetic interactions have been shown utilizing muon-spin rotation,[3] electron-spin-resonance (ESR) techniques,[8] and Raman[9] and far-infrared experiments.[10]

Focusing on the Gd compound, the structural details were reported by McLaughlin *et al.*[11] and Chmaissem *et al.*[12] The average structure is tetragonal, but superstructures resulting from coherent rotations of the RuO$_6$ octahedra were observed by electron diffraction.[11] The RuO$_6$ octahedra are rotated around the c axis, with a small additional rotation around an axis perpendicular to c. Specifically the superconducting properties sensitively depend on sample-preparation procedures. But a clear correlation between structural details and superconducting transition temperatures has not yet been established. Even nonsuperconducting samples reveal the same tetragonal space group $P4/mmm$ with lattice parameters $a = 0.3833$ nm and $c = 1.159$ nm,[13] similar to those observed in the superconducting compounds with $a = 0.3836$ nm and $c = 1.156$ nm,[12] and $a = 0.3838$ nm and $c = 1.157$ nm.[11] Finally, using isotope-enriched samples it has been proven that the Ru atoms order antiferromagneti-cally (G type) along the c axis with a saturated moment of $1.2\mu_B$ and with the neighboring spins being antiparallel in all three crystallographic directions.[14,15] The ferromagnetic moment which has been observed in magnetization measurements must result from the rotation of the Ru octahedra about an axis perpendicular to c, resulting in finite antisymmetric exchange interactions and probably producing a slight canting of the Ru moments. From the neutron diffraction an upper limit of $0.1\mu_B$ was derived for the ferromagnetic moment.[14] The Gd moments order independently below 2.5 K, again revealing simple G-type antiferromagnetism.[14] It is important to note that the Gd spins are surrounded by four Ru spins with a spin structure that yields a complete cancellation of an average interaction between Ru and Gd. However any ferromagnetic moment at the Ru site would induce a ferromagnetic moment at the Gd site suppressing this frustration.[15]

The coexistence of superconductivity and weak ferromagnetism motivated proposals of unconventional superconducting order parameters.[16–19] That the order parameter may be of the Fulde-Ferrell-Larkin-Ovchinnikov type has been derived from band-structure calculations by Pickett *et al.*[16] who calculated a ferromagnetic ground state using local-density approximation + U methods. On the contrary, Nakamura *et al.*[20] derived an antiferromagnetic ground state using first-principles full-potential linearized augmented plane-wave calculations. And even the old ideas put forth by Anderson and Suhl[21] about the possibility of a domainlike magnetic structure in the presence of superconductivity, the so-called cryptoferromagnetic state, comes to mind. In order to gain further insight into the interplay of magnetism and superconductivity we synthesized a number of doped Ru(Sr$_{1-x}$La$_x$)$_2$GdCu$_2$O$_8$ compounds with La concentrations ranging from $0 < x < 0.1$. The samples were carefully characterized using x-ray diffraction and were investigated using susceptibility, magnetization, and electrical transport measurements.

II. EXPERIMENTAL DETAILS

Single-phase polycrystalline Ru(Sr$_{x-1}$La$_x$)$_2$GdCu$_2$O$_8$ samples were prepared using conventional ceramic techniques. The samples have been synthesized by solid-state reaction methods. High-purity RuO$_2$, SrCO$_3$, La$_2$O$_3$, Gd$_2$O$_3$, and CuO powders were mixed in an appropriate ratio and calcinated at 960 °C in air. The product was then ground, pressed into pellets, and heated at 1010 °C in a nitrogen atmosphere. The pellets were then reground into fine powders and put into a furnace at 1050 °C for 10–12 h in flowing oxygen, followed by slow cooling. This sintering was repeated twice at temperatures of 1055 °C and 1060 °C with intermediate grindings. Finally the samples were again pressed into pellets and annealed for 6 days at 1060 °C in flowing oxygen and cooled slowly at the rate of 30 °C/h to room temperature. Some of the samples were annealed further for 6 days under the same conditions to see how the sample quality increases on further heat treatments. Characterization of Ru(Sr$_{1-x}$La$_x$)$_2$GdCu$_2$O$_8$ by powder x-ray diffraction at room temperature revealed the same primitive tetragonal structure of pure RuSr$_2$GdCu$_2$O$_8$ for all samples investigated ($x = 0$, 0.01, 0.03, 0.05, and 0.1). This structure is characterized by space group $P4/mmm$ in which Ru ions occupy the crystallographic $1b$ site $(0,0,\frac{1}{2})$, Gd ions the $1c$ site $(\frac{1}{2},\frac{1}{2},0)$, Sr and La ions occupy the Wyckoff position $2h$ $(\frac{1}{2},\frac{1}{2},z)$, Cu the $2g$ position $(0,0,z)$, and the oxygen ions are distributed among the $8s$ $(x,0,z)$, the $4o$ $(x,\frac{1}{2},\frac{1}{2})$, and the $4i$ $(0,\frac{1}{2},z)$ positions. The crystallographic structure is closely related to that of other 1212-type cuprate superconductors. Planes of RuO$_6$ octahedra are connected via their apical oxygen ion with layers of CuO$_5$ square pyramids. Note that the bond angle ϕ of Ru-O-Cu ions, which is characteristic for distortions of the RuO$_6$ ocatheda, is essential for the magnetic exchange interaction and the charge transfer between the Ru-O and Cu-O layers. This angle ϕ signals the rotation of the RuO$_6$ octahedra around an axis perpendicular to the c axis.

Exemplarily, the x-ray diffraction patterns of Ru(Sr$_{1-x}$La$_x$)$_2$GdCu$_2$O$_8$ for $x = 0$, $x = 0.03$, and $x = 0.1$ are shown in Fig. 1. As evident from Fig. 1, the intensities decrease for increasing La concentration due to increasing absorption. Consequently, the less accurate statistics upon increasing the La concentration are mainly responsible for increasing reliability factors. For all compounds investigated no significant spurious phases could be detected. For $x = 0$ and $x = 0.1$ a weak intensity just above the sensitivity level of the experiment can be detected close to $2\Theta \approx 31.5°$. Usually this intensity is attributed to residues of SrRuO$_3$ or GdCuO$_4$.[22] These compounds both reveal magnetic order with ordering temperatures close to 165 K and 260 K, respectively. No anomalies could be detected in the magnetization experiments close to these temperatures. The results of the refinements of the x-ray-diffraction patterns are summarized in Table I. For the pure compound the lattice parameters determined in this work compare well with those reported in literature,[11,12] and also the atomic positions which
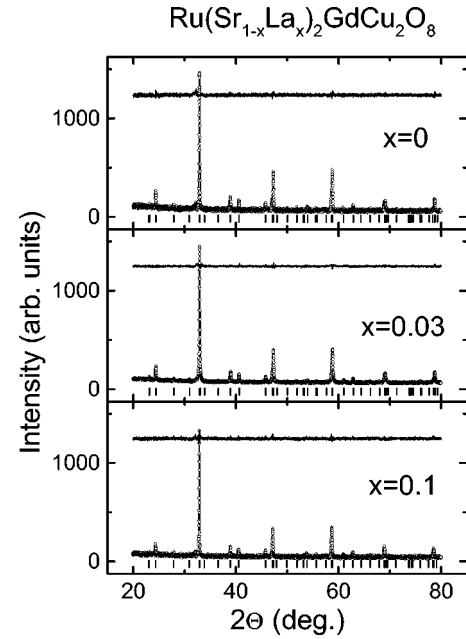

FIG. 1. X-ray-diffraction spectra of Ru(Sr$_{1-x}$La$_x$)$_2$GdCu$_2$O$_8$ for $x = 0$, 0.3, and 0.1 at room temperature. The lines at the bottom of the diagram denote the peak positions due to the $P4/mmm$ space group. The results of the Rietveld analyses are indicated as solid lines. The difference patterns are indicated at the top of each pattern.

can be refined according to the crystal symmetry agree well with published results.[11] With increasing La doping only insignificant changes of the lattice parameters can be observed. Even the Cu-O-Ru bond angle $\phi \approx 171°$, for the compounds investigated, remains rather constant. Hence we expect that the charge transfer from Cu to Ru remains the same. But of course, the holes are compensated for by the extra electrons induced via the La doping and, at first sight, disorder only is introduced off the RuO$_2$ and CuO$_2$ layers. One might speculate whether La^{3+} really replaces Sr^{2+} or rather is substituted for Gd^{3+}. Our main experimental evidence comes from the careful Rietveld analyses which revealed the best agreement between observed and calculated intensities in the case in which Sr is indeed replaced by La. We are aware that diffraction experiments are not very sensitive to low impurity levels and probably yield no finite proof. However we believe that at least for the sample with $x = 0.1$, the Rietveld refinement which signals a La concentration of 11.8% is significant and certainly can be considered as strong experimental evidence. In addition, if La replaces Gd the samples would contain an excess of up to 20% of gadolinium-rich impurity phases, for which we found no indications, neither in the diffraction patterns nor in preliminary electron-paramagnetic-resonance experiments which should be rather sensitive even to low Gd concentrations.

The measurements of the magnetic ac susceptibility and the magnetization were carried out using a Quantum Design Superconducting quantum interference device magnetometer which operates in fields up to 50 kOe, for temperatures 1.8 K $< T <$ 800 K, and with a mutual induction bridge for ac-susceptometry and dc-extraction magnetization measure-

TABLE I. Crystallographic properties of $RuSr_{2(1-x)}La_{2x}GdCu_2O_8$ ($x=0$, 0.01, 0.03, 0.05, 0.1) as obtained by Rietveld refinements of powder x-ray-diffraction patterns recorded at room temperature. Listed are the lattice constants $a(=b)$ and c, the cell volume V, the Wyckoff positions and their corresponding positional parameters (for atoms with refinable positional parameters only), the angle ϕ of the Cu-O-Ru bond, the La concentration as determined from the refined occupancy values, and the Bragg reliability factors R_{Bragg} of the crystallographic structures.

x	0	0.01	0.03	0.05	0.1
a (Å)	3.8399	3.8397	3.8407	3.8444	3.8473
c (Å)	11.5766	11.5708	11.5662	11.5583	11.5657
V (Å^3)	170.70	170.59	170.61	170.82	171.19
Sr ($\frac{1}{2},\frac{1}{2},z$)	$z=0.3108$	$z=0.3112$	$z=0.3104$	$z=0.3112$	$z=0.3100$
Cu (0, 0, z)	$z=0.1484$	$z=0.1462$	$z=0.1511$	$z=0.1496$	$z=0.1498$
O$_1$ (x,0,z)	$x=0.0417$	$x=0.0564$	$x=0.0176$	$x=0.0482$	$x=0.0383$
	$z=0.3375$	$z=0.3321$	$z=0.3407$	$z=0.3281$	$z=0.3368$
O$_2$ ($0,\frac{1}{2},z$)	$z=0.1228$	$z=0.1252$	$z=0.1263$	$z=0.1165$	$z=0.1250$
O$_3$ ($x,\frac{1}{2},\frac{1}{2}$)	$x=0.1174$	$x=0.1356$	$x=0.1568$	$x=0.1277$	$x=0.1378$
ϕ (°)	171	168	174	170	172
La concentration (%)		1.0 (fixed)	4.2	4.9	11.8
R_{Bragg} (%)	5.86	4.78	5.75	5.55	7.30

ments within an Oxford cryo-magnet in fields up to 140 kOe and in the temperature range 1.5 K$<T<$300 K. The transport investigations were carried out in the same Oxford system. dc resistance and magnetoresistance have been recorded employing a standard four-probe method.

III. RESULTS AND DISCUSSION

A. dc resistivity

Figure 2 shows the dc resistivity of $Ru(Sr_{1-x}La_x)_2GdCu_2O_8$ vs temperature at zero external field as observed for the complete series of samples investigated. The main frame compares the results for the pure compound with those obtained in the La-doped compounds with $x=0.01$, 0.03, and 0.05. Focusing on the pure compound, on decreasing temperatures the resistivity decreases, passes through a minimum close to 80 K, and slightly increases just before the onset of superconductivity at 50 K, while the resistance completely has vanished below 31 K. The temperatures where the resistance reaches 90% and 10% of the initial onset values amount to 46 and 35.5 K, respectively, yielding a smeared-out superconducting phase transition of 10 K which seems to be rather broad even for ceramic samples. On La doping the room-temperature resistivity values are continuously increased. The sample with $x=0.01$ behaves similarly to the pure compound with the superconducting phase transition shifted to values which are approximately 10 K lower. For $x\geqslant0.03$ superconductivity is fully suppressed. Again the resistivity passes through a minimum and reveals a semiconducting temperature characteristic below 100 K. Finally for $x=0.1$, $\rho(T)$ is strongly increased even at room temperature and increases for all temperatures below 300 K (see solid line in the inset of Fig. 2). In this inset we also show the resistivity for $x=0.1$ in an Arrhenius-type representation (dashed line) to demonstrate that the strong increase towards low temperatures is not a

purely thermally activated behavior. But the resistivity in this compound also cannot be described using variable-range-hopping models which consider the hopping of charge carriers in strongly disordered semiconductors. The magnetic phase transition appears as a weak smeared-out anomaly in the temperature dependence of the resistivity at temperatures close to 150 K. This broad anomaly shifts to higher temperatures on increasing x.

As an example of the magnetic-field dependence of the resistivity in the superconducting state, Fig. 3 shows the temperature dependence of the resistivity for the pure compound in zero external field and in fields of 100 kOe (upper frame
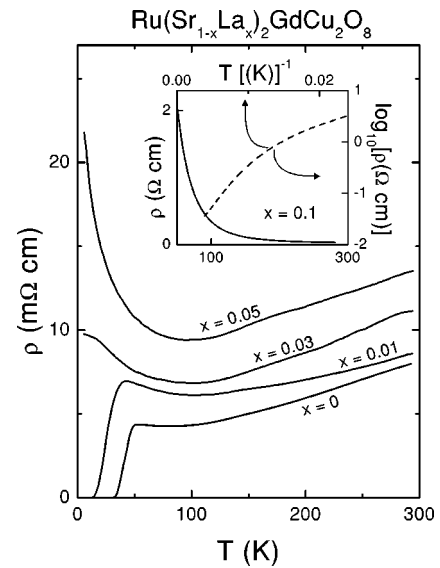

FIG. 2. Electrical resistance vs temperature in $Ru(Sr_{1-x}La_x)_2GdCu_2O_8$ for La concentrations $x=0$, 0.01, 0.03, and 0.05. The resistivity for $x=0.1$ is shown in the inset: ρ vs T (solid line, left, and lower scale) and $\log\rho$ vs T^{-1} (dashed line, right, and upper scale).
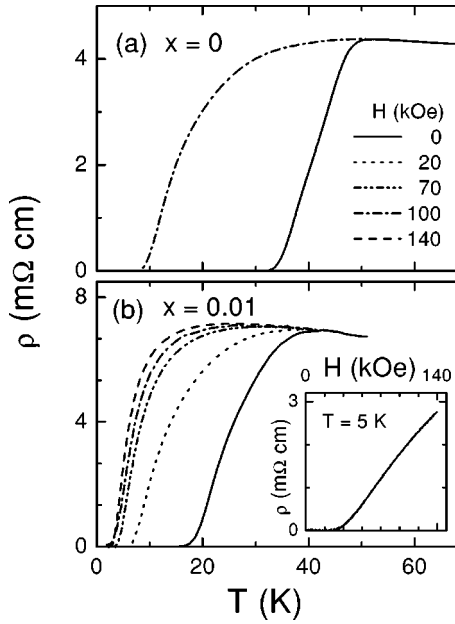
FIG. 3. dc resistivity versus temperature for $x=0$ (a) and $x=0.01$ (b) for magnetic fields as indicated in the figure. The inset in (b) illustrates the magnetic-field dependence of samples with $x=0.01$ at $T=5$ K.

of Fig. 3) and for $x=0.01$ for a series of external magnetic fields $0<H<140$ kOe (Fig. 3, lower frame). In both samples the superconducting transition temperatures are significantly shifted to lower temperatures. But at the lowest temperatures even in the highest fields the samples remain superconducting. The inset in Fig. 3 reveals the magnetic-field dependence of the resitivity for $x=0.01$ at 5 K. The electrical resistance approaches zero values at a field of approximately 3 T.

B. Magnetization and magnetic susceptibility

1. RuSr$_2$GdCu$_2$O$_8$

Before studying magnetization and susceptibility as a function of La doping we investigate the pure compound in some detail. Here special attention is paid to investigate the ferromagnetic character of the magnetic order. From neutron scattering it has become clear[14,15] that the Ru ions display predominantly a *G*-type antiferromagnetic structure, with a ferromagnetic moment below $0.1\mu_B$. The temperature dependencies of the magnetic dc susceptibility $\chi_{dc}=M/H$ (upper frame) and of the inverse dc susceptibility (lower frame) are shown in Fig. 4. The M/H data were measured at $H=10$ kOe and thus the onset of the ferromagnetic order parameter (spontaneous magnetization) at $T_m\approx140$ K already is smeared out. The solid line in the upper frame gives the ac susceptibility measured at a small ac field of $H_{ac}\approx0.1$ Oe$_{rms}$. Here a pronounced peak is detected at T_m. The peak is followed by a plateaulike regime towards lower temperatures. This type of behavior is typical for domain contributions below the order temperature in soft ferromagnets. But it is worth mentioning that the maximum value of χ'_{ac} at the transition is relatively small compared with other

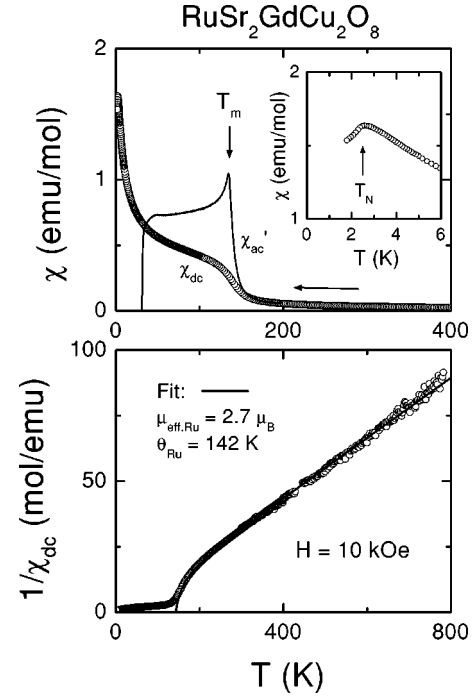FIG. 4. Temperature dependence of the dc susceptibility $\chi_{dc}=M/H$ (upper frame, open circles) and the inverse susceptibility $1/\chi_{dc}$ (lower frame, open circles) measured on cooling at $H=10$ kOe for temperatures 1.8 K$<T<$800 K. The inset in the upper frame is a magnification of the low-temperature behavior of χ_{dc}. The solid line in the upper frame represents the ac susceptibility measured with a stimulus of $H=0.1$ Oe$_{rms}$ at a frequency of $\nu=1$ kHz. The solid line in the lower frame represents a fit according to the superposition of two Curie-Weiss contributions as described in the text with the parameters given in the table (μ_{eff}: effective paramagnetic moment; θ: effective mean-field interaction of the corresponding sublattice).

ferromagnets. $4\pi\chi_{ac}<0.13$ emu/cm^3, i.e., nearly no demagnetization effects are present even in the vicinity of the magnetic transition.

At temperatures below 50 K the dc magnetization shows a Curie-like increase and finally a small peak at $T_N\approx2.7$ K (see inset of Fig. 4), which signals the antiferromagnetic order of the Gd sublattice. The overall behavior of the dc magnetization at $H=10$ kOe can be described assuming two independent contributions of the Gd and the Ru sublattices, respectively. The Ru sublattice orders (weak) ferromagnetically at T_m while Gd remains paramagnetic and orders antiferromagnetically at low temperatures. The lower frame of Fig. 4 shows the inverse dc susceptibility in the temperature range 1.5 K$<T<$800 K. The solid line is fitted according to the superposition of two independent Curie-Weiss contributions. (The fitting regime only included the linear, i.e., field-independent, temperatures, where χ'_{ac} and χ_{dc} coincide). The parameters for the Gd sublattice were kept fixed at the values $\mu_{eff}=7.94\mu_B$ and $\theta=-4$ K corresponding to the $4f^7$-electron configuration of Gd ($J_{Gd}=7/2$) and the low antiferromagnetic order temperature. The resulting fitting parameters for the Ru sublattice are given in Fig. 4 and Table II. The effective moments resulting from this fitting proce-

TABLE II. Magnetic properties of $RuSr_{2(1-x)}La_{2x}GdCu_2O_8$ (x = 0, 0.01, 0.03, 0.05, 0.1). The parameters were obtained by fitting the inverse magnetic-susceptibility data as shown in the inset of Fig. 8 below, employing two independent Curie-Weiss contributions from the Ru and the Gd sublattices, respectively. The parameters $\theta_{Gd} = -4$ K and $\mu_{eff,Gd} = 7.94$ were kept fixed.

x	0	0.01	0.03	0.05	0.1
μ_{eff} (μ_B)	2.7	2.8	2.8	2.4	2.4
θ_{Ru} (K)	142	142	154	180	185

dure turned out to be enhanced compared to the ones expected for a low-spin (LS) $4d^3$-electron configuration in Ru^{5+} ($S_{Ru,LS} = 1/2 \rightarrow \mu_{eff} = 1.73\mu_B$) and the Curie-Weiss temperature of the Ru sublattice is somewhat larger than the magnetic ordering temperature. Similar evaluations can be found in literature.[3,6] As has been pointed out by Butera *et al.*,[6] by fixing some of the parameters significantly, different parameters can evolve. Using four free parameters for both sublattices one gains a value of $\mu_{eff} = 1.9\mu_B$ for the Ru effective moment together with an enhanced Curie-Weiss temperature for the Gd contribution of $\theta_{Gd} \approx 20$ K. Probably one should not overemphasize the validity of the fitting parameters which are highly correlated, and we have to admit that the resulting fit parameters as indicated in Fig. 4 are in some ways ambiguous. As mentioned above, the paramagnetic moment of Ru seems to be slightly larger, as expected for a LS configuration of Ru^{5+}. From NMR (Ref. 18) and x-ray appearance near-edge structure experiments (cited after Ref. 6) a mixed-valence state of Ru^{5+} ($S = 3/2$) and Ru^{4+} ($S = 1$) has been deduced yielding an effective moment of the order of $\mu_{eff} \approx 3\mu_B$. However, taking into account the field-dependent magnetization data (see below) strongly supports the $S = 1/2$ state for Ru due to a saturation value of $M_s = 8\mu_B$/f.u. ($7\mu_B$ from Gd, $1\mu_B$ from Ru).

Even more striking evidence for the picture of a ferromagnetic Ru moment within a paramagnetic Gd background is given in Fig. 5. Here $M(H)$ curves in magnetic fields up to 140 kOe are shown for several temperatures as denoted in the figure. The solid lines are calculated employing again two independent Brillouin functions for the Ru and Gd sublattices. The values for spin states of Gd ($J_{Gd} = 7/2$) and Ru ($S_{Ru, LS} = 1/2$), as well as the effective coupling within the Ru lattice $\theta_{Ru} = 146$ K and the effective Gd-Gd interaction $\theta_{Gd} = -4$ K, were kept fixed. The data can well be described with this simple model for fields $H \geqslant 10$ kOe. For small fields, of course, a discrepancy between the fits and the data has to be expected because the measurements exhibit only a very weak remanent magnetization, which together with a finite coercive field rises below $T \approx 50$ K (see inset of Fig. 5). The values for the coercivity field and the remanent magnetization at $T = 1.8$ K of $H_{coer} \approx 350$ Oe and $M_r \approx 0.15\mu_B$/Ru are much smaller than, e.g., in the ferromagnet $RuSrO_3$. The low magnetization and susceptibility responses at low fields and below T_m coincide with results from neutron-diffraction measurements, which in this regime denote a G-type antiferromagnetic order of the Ru sublattice with a small ferromagnetic component of less than
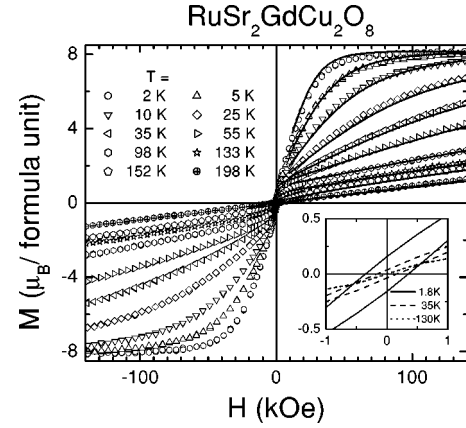

FIG. 5. Hysteresis loops of the dc magnetization measured at various temperatures as denoted in the figure. The solid lines represent fits employing two independent Brillouin functions as described in the text. The inset illustrates the development of coercitivity and remanent magnetization towards low temperatures.

$\approx 0.1\mu_B$/Ru.[14,15] At higher external magnetic fields a purely ferromagnetic state is induced. As can be seen in Fig. 5 the saturation value of $M_s = 8\mu_B$/f.u. unit is reached, in agreement with the expectation for localized ferromagnetically aligned Gd^{3+} and Ru^{5+} spins. Ferromagnetism is induced already for fields smaller than 10 kOe.

In Fig. 6 the real part of the ac susceptibility χ_{ac} is plotted against the dc bias field H_{dc} for several temperatures in the magnetically ordered phase regime. The data were taken after zero-field cooling from above T_m to the respective temperatures and then measured at $\nu = 1$ Hz with $H_{ac} = 1$ Oe. In the whole temperature range below T_m distinct maxima can be detected in $\chi'_{ac}(H_{dc})$. Usually such features are referred to as a metamagnetic transition. A purely ferromagnetic state would result in a monotonous decrease of the susceptibility with increasing magnetic field. For a canted
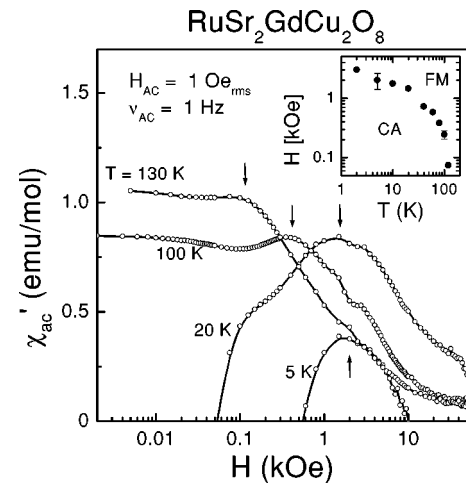

FIG. 6. Field dependence of the real part of the ac susceptibility for $RuSr_2GdCu_2O_8$ at different temperatures below T_m. The arrows indicate a characteristic temperature where a metamagnetic transition occurs. The inset shows a schematic (H,T) phase diagram separating a canted (CA) and a purely ferromagnetic (FM) phase.
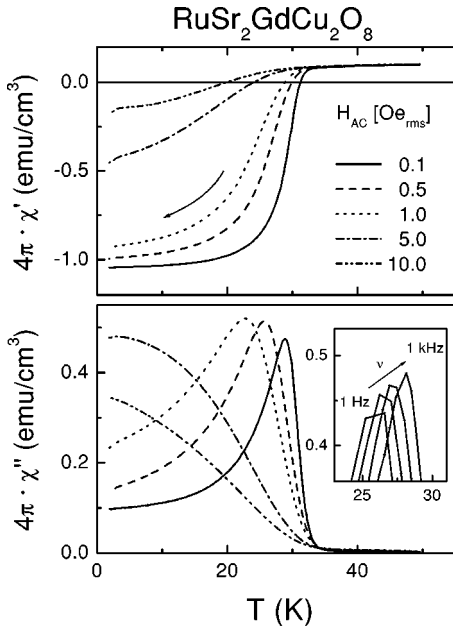
RuSr$_2$GdCu$_2$O$_8$

FIG. 7. Real part (upper frame) and imaginary part (lower frame) of the complex volume ac susceptibility measured at ν =1 kHz for various stimulation amplitudes H_{ac}. The data were taken under cooling in zero external field. The inset in the lower field shows $\chi''(T)$ in the vicinity of the peak for frequencies 1 Hz $\leq \nu \leq 1$ kHz measured with $H_{ac}=0.1$ Oe$_{rms}$.

antiferromagnetic state one would expect a nearly constant behavior because of the continuous enhancement of the canting angle due to the external field. For the superconducting state, of course, a negative value for χ'_{ac} is observed. χ'_{ac} turns positive when the increasing field flux penetrates the superconducting sample and gives a positive contribution. The results shown in Fig. 6 can qualitatively be interpreted within this picture of a field-induced transition from a canted (CA) antiferromagnetic to a ferromagnetic (FM) state. In the neutron-scattering experiments[14] a spin-flop transition of the Ru moments has been observed close to 4 kOe at 80 K. This is significantly higher when compared to our results. The inset of Fig. 6 shows the positions of the maxima in $\chi'_{ac}(H_{dc})$ and illustrates the regime where the (CA) antiferromagnetic state is stable. In our ac-susceptibility results at 50 K a FM state is established in fields as low as 1 kOe.

In order to study the magnetic properties within the superconducting phase, we performed a series of ac susceptibility measurements in the temperature range 1.8 K$<T$ <50 K with frequencies 1 Hz$<\nu<1$ kHz and ac field amplitudes of 0.1 Oe$_{rms}<H_{ac}<10$ Oe$_{rms}$ as illustrated in Fig. 7. The data were received on cooling in zero external dc field. The real part of the susceptibility χ'_{ac} (upper frame of Fig. 7) shows a significant drop undergoing the superconducting transition and becomes negative close to the temperatures where the electrical resistance approaches zero. For small field amplitudes (0.1 Oe$_{rms}$, solid lines in Fig. 7) the sample is fully screened and a value close to $\chi'_{ac,volume}=-1/4\pi$ emu/cm^3 is reached. It has to be stated that the ac method is no proof of the Meissner effect, which has controversially been discussed for this system. $\chi''_{ac}(T)$ (lower frame of Fig.

7) shows a broad peak which coincides with an inflection point in χ'_{ac}. The onset of the drop in χ'_{ac} lies close to the temperature where the resistivity approaches zero (see Fig. 2) and at this temperature also the losses in χ''_{ac} strongly increase. Sometimes in polycrystalline high-T_c superconductors two loss peaks can be distinguished due to the intrinsic (intragrain) lower critical field and lower critical field of the intergrain region. In this case only one contribution can be resolved. At low temperatures and small external fields which are smaller than the lower critical field $H_{ac}\ll H_{c1}$, the sample should be completely screened and the real part of the susceptibility $\chi'_{ac}=-1/4\pi$ emu/cm^3 while the losses χ''_{ac} should vanish. On the other hand, close below the intrinsic superconducting transition temperature the stimulus exceeds the lower critical field $H_{ac}\gg H_{c1}$ and the sample will nearly completely be penetrated, which results in a vanishing contribution to complex χ^*_{ac}. Between these extremes the sample will be partially penetrated resulting in a diamagnetic contribution to χ'_{ac} and finite loss contributions χ''_{ac} due to the hysteresis effect of the flux trapped in the sample. Within this scenario for an ordinary type-II superconductor the peak in $\chi''_{ac}(T)$ would denote the case in which the applied field and the effective lower critical field are of the same order of magnitude $H_{ac}\approx H_{c1}$. In the present case it is remarkable that even for the lowest temperatures and smallest applied ac fields (see solid line in the lower frame of Fig. 7) the loss does not vanish, as expected for the case $H_{ac}\gg H_{c1}$, but seems to saturate at a finite value. This means that even at $T=2$ K and $H_{ac}=0.1$ Oe$_{rms}$ a considerable fraction of the sample is penetrated by magnetic flux.

In addition these features in the ac susceptibility reveal a distinct frequency dependence. Such effects may be explained by the viscosity of the vortices due to flux pinning. The frequency dependence of the peak in $\chi''_{ac}(T)$ measured with $H_{ac}=0.1$ Oe$_{rms}$ (shown in inset of Fig. 7) can be described using an Arrhenius law $\nu=\nu_0 \exp(-E_b/T)$ with an effective pinning barrier of $E_b\approx 0.21$ eV. This value is one order-of-magnitude smaller than found, e.g., in YBa$_2$Cu$_3$O$_{7-\delta}$ (YBCO) for the same stimulus.

Both the vanishing H_{c1} and the low pinning barrier may result from the enhancement of the applied external fields by the intrinsic ferromagnetic magnetization. The internal fields seem to be even always larger than an "intrinsic" H_{c1}, which would result in a spontaneous vortex phase.[23]

2. Ru(Sr$_{1-x}$La$_x$)$_2$GdCu$_2$O$_8$

Figure 8 shows the dc magnetization as obtained for the pure and the La-doped compounds in an external magnetic field of 0.5 Oe. The field-cooled (FC) results reveal that the small ordered moment of the pure compound even decreases on La doping. This fact implies that the canting angle for the doped compounds almost approaches 180° and is not correlated with the Cu-O-Ru angle, which remains constant within experimental uncertainties (see Table I).

For $x=0$ and $x=0.01$ we observed a clear splitting of the FC and zero-field cooled (ZFC) branches close to T_m, which is absent for the higher-doping concentrations. From the FC/ ZFC measurements at $H_{dc}=0.5$ Oe we found evidence at
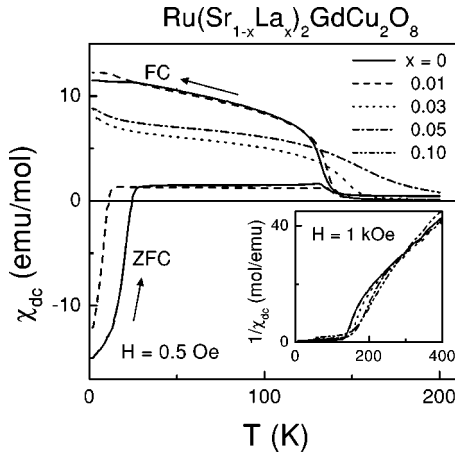
FIG. 8. dc susceptibility versus temperature for $Ru(Sr_{1-x}La_x)_2GdCu_2O_8$ for La concentrations $x = 0$, 0.01, 0.03, and 0.1 as measured in an external magnetic field of 0.5 Oe. For $x = 0$ and 0.01 the FC and ZFC branches are shown. The inset shows the inverse of the susceptibility in a temperature range up to 400 K.

least for a partial evolution of the Meissner state. The diamagnetic contribution of the FC magnetization curve can be estimated to amount to 5% of the ZFC value. But there is no evidence for the complete absence of the Meissner effect as proposed in literature. In the inset of Fig. 8 we show the inverse susceptibility also for the La-doped samples. Already a first inspection reveals that the magnetic transition temperature significantly is shifted to higher temperatures on increasing doping. If we analyze the data as outlined above and as shown in Fig. 4 we find an increase of the Curie-Weiss temperature of the Ru sublattice to values of 160 K for $x = 0.05$ and 180 K for $x = 0.1$. This significant increase in the exchange interaction can only be explained assuming that the superexchange is enhanced via structural changes induced by the La doping. As the lattice constants almost remain constant for all doping levels investigated one possibly has to assume slight changes in the bond angles.

Similar to the magnetization measurements in the pure compound (Fig. 5), Fig. 9 documents $M(H)$ for $Ru(Sr_{0.97}La_{0.03})GdCu_2O_8$ for a series of temperatures below and above the magnetic ordering temperature $T_m = 155$ K. Again the experimental results can be satisfactorily described assuming two independent Brillouin functions for the Ru and the Gd sublattices with $J_{Gd} = 7/2$, $S_{Ru, LS} = 1/2$, $\Theta_{Ru} = 154$ K, and $\Theta_{Gd} = -4$ K. These values were kept fixed and the solid lines in Fig. 9 represent calculations with this set of parameters. When compared to the results on pure Ru-1212, in the La-doped sample only, the Ru-Ru exchange interaction is slightly enhanced. Results on the real part of the ac susceptibility χ'_{ac} for $Ru(Sr_{0.97}La_{0.03})GdCu_2O_8$ are plotted in Fig. 10. Like in the pure compound the data were taken after zero-field cooling from above T_N and were measured at 1 Hz with an ac field of 1 Oe. Maxima in the field dependence of χ'_{ac} can still be detected and signal a metamagnetic phase transition. The corresponding phase diagram, where the solid points separate a ferromagnetic phase at high fields from a canted phase at low fields, is shown in the inset
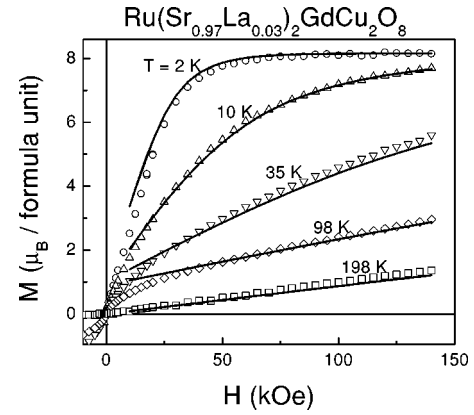

FIG. 9. dc magnetization and $M(H)$ measured at different temperatures below and above the magnetic ordering temperature in $Ru(Sr_{0.97}La_{0.03})GdCu_2O_8$. The solid lines have been calculated using two independent Brillouin functions for the Ru and Gd sublattices with the parameters as described in the text.

of Fig. 10. In clear distinction to the observations in the pure compound, the low-field susceptibility steadily increases on decreasing temperatures, indicating that the sample reveals no traces of superconductivity.

IV. CONCLUSIONS

We have presented a detailed investigation of the structural and electronic properties of pure and La-doped $RuSr_2GdCu_2O_8$. Up to La concentrations $x = 0.1$ the structural details almost remain unchanged, including the $Cu-O_1$ bond lengths and the $Cu-O_1-Ru$ bond angles. It has been pointed out by McLaughlin et al.[11] that the $Cu-O_1$ bond is unusually short when compared to other cuprate superconductors and results in a charge transfer introducing p holes in the CuO_2 planes and electrons into the t_{2g} band of the RuO_2 layers. Based on simple valence-bond caculations the oxida-
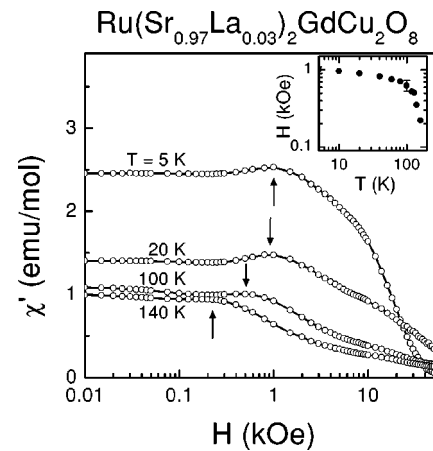

FIG. 10. Field dependence of the real part of the ac susceptibility for $Ru(Sr_{0.97}La_{0.03})GdCu_2O_8$ at various temperatures below T_m. The arrows indicate the characteristic temperatures where the metamagnetic transition occurs at a given temperature. The inset shows a schematic phase diagram separating the canted (CA) from the ferromagnetic (FM) phases.

tion states of Cu and Ru can be written as $2+p$ and $5-2p$, respectively.[24] Using the structural data, p can be estimated for all compounds investigated and scatters around values $p \approx 0.45$ which is much too high regarding the closeness of the metal-to-insulator transition. We would like to recall that in optimally doped $YBa_2Cu_3O_7$, $p \approx 0.2$.[24] Already 3% of La^{3+} substitution for Sr^{2+} completely suppresses superconductivity which means that in addition to the charge compensation the remaining holes are trapped, possibly by disorder effects. Nevertheless, this effect reveals that $RuSr_2GdCu_2O_8$ is very close to a metal-to-insulator transition and the concentration of holes in the CuO_2 planes must be very low.

Similar doping experiments with a heterovalent substitution have been performed by Klamut *et al.*[25] These authors substituted Ce^{4+} for Gd^{3+} and hence doped electrons into the system, as we did in this work, substituting La^{3+} for Sr^{2+}. Also in the Ce-doped samples superconductivity is strongly suppressed and already 5% Ce in Ru-1212 yields a nonsuperconducting material. In addition the magnetic ordering temperature increases slightly, similar to our observations.

From the magnetic susceptibility it is clear that there is a very moderate canting of the Ru moment, yielding only weak ferromagnetism. On doping, the onset of magnetic order is shifted to higher temperatures, but the ferromagnetic component even becomes weaker, pointing towards a more ideal antiferromagnetic G-type structure. This point also illuminates a severe problem which exists in the pure compound. Two thermodynamic phase transitions according to ordering of the two sublattices can only occur if they are fully decoupled. A weak ferromagnetic component certainly will couple the Ru and Gd spins and indeed in electron-spin-resonance experiments a finite coupling has been detected.[8] Of course ESR experiments are carried out in finite fields which according to Fig. 6 immediately will induce a ferromagnetic state. However, many experimental facts point toward a ferromagnetic component in zero external field and one expects only one magnetic phase transition. However, definitely two transitions can be detected (Fig. 4). This fact remains to be explained.

From ac-susceptibility experiments we provide a schematic (H,T) phase diagram for the pure compound and the sample doped with 3% La separating a CA phase at low fields from a induced FM state at higher external fields. Finally we discuss the ac-susceptibility results in terms of a spontaneous vortex phase.

[1] I. Felner, U. Asaf, Y. Levi, and O. Millo, Phys. Rev. B **55**, R3374 (1997).

[2] J. L. Tallon, C. Bernhard, M. E. Bowden, P. W. Gilberd, T. M. Stoto, and D. Pringle, IEEE Trans. Appl. Supercond. **9**, 1696 (1999).

[3] C. Bernhard, J. L. Tallon, Ch. Niedermayer, Th. Blasius, A. Golnik, E. Brücher, R. K. Kremer, D. R. Noakes, C. E. Stronach, and E. J. Ansaldo, Phys. Rev. B **59**, 14 099 (1999).

[4] J. L. Tallon, J. W. Loram, G. V. M. Williams, and C. Bernhard, Phys. Rev. B **61**, R6471 (2000).

[5] C. Bernhard, J. L. Tallon, E. Brücher, and R. K. Kremer, Phys. Rev. B **61**, R14 960 (2000).

[6] A. Butera, A. Fainstein, E. Winkler, and J. L. Tallon, Phys. Rev. B **63**, 054442 (2001).

[7] G. V. M. Williams and S. Krämer, Phys. Rev. B **62**, 4132 (2000).

[8] A. Fainstein, E. Winkler, A. Butera, and J. L. Tallon, Phys. Rev. B **60**, R12 597 (1999).

[9] A. Fainstein, P. Etchegoin, H. J. Trodahl, and J. L. Tallon, Phys. Rev. B **61**, 15 468 (2000).

[10] A. Boris, P. Mandal, C. Bernhard, N. N. Kovaleva, K. Pucher, J. Hemberger, and A. Loidl, Phys. Rev. B **63**, 184505 (2001).

[11] A. C. McLaughlin, W. Zhow, J. P. Attfield, A. N. Fitch, and J. L. Tallon, Phys. Rev. B **60**, 7512 (1999).

[12] O. Chmaissem, J. D. Jorgensen, H. Shaked, P. Dollar, and J. L. Tallon, Phys. Rev. B **61**, 6401 (2000).

[13] I. Felner, U. Asaf, S. Reich, and Y. Tsabba, Physica C **311**, 163 (1999).

[14] J. W. Lynn, B. Keimer, C. Ulrich, C. Bernhard, and J. L. Tallon, Phys. Rev. B **61**, R14 964 (2000).

[15] J. D. Jorgensen, O. Chmaissem, H. Shaked, S. Short, P. W. Klamut, B. Dabrowski, and J. L. Tallon, Phys. Rev. B **63**, 054440 (2001).

[16] W. E. Pickett, R. Weht, and A. B. Shick, Phys. Rev. Lett. **83**, 3713 (1999).

[17] Jion-Xin Zhn, C. S. Ting, and C. W. Chu, Phys. Rev. B **62**, 11 369 (2000).

[18] K. Kumagai, S. Takada, and Y. Furukawa, Phys. Rev. B **63**, 180509 (2001).

[19] C. W. Chu, Y. Y. Xue, R. L. Meng, J. Cmaidalka, L. M. Dezaneti, Y. S. Wang, B. Lorenz, and A. K. Heilman, cond-mat/9910056 (unpublished).

[20] K. L. Nakamura, K. T. Park, A. J. Freeman, and J. D. Jorgensen, cond-mat/0010227 (unpublished).

[21] P. W. Anderson and H. Suhl, Phys. Rev. **116**, 898 (1959).

[22] M. Hrovat, A. Becan, Z. Samardzija, J. Holc, A. Brglez, and D. Mihailovic, J. Mater. Sci. Lett. **19**, 919 (2000).

[23] E. B. Sonin and I. Felner, Phys. Rev. B **57**, R14 000 (1998).

[24] R. J. Cava, A. W. Hewat, E. A. Hewat, B. Batlogg, M. Marezio, K. M. Rabe, J. J. Krajewski, W. F. Peck, Jr., and L. W. Rupp, Jr., Physica C **65**, 419 (1990); J. L. Tallon, *ibid.* **168**, 85 (1990).

[25] P. W. Klamut, B. Dabrowski, J. Mais, and M. Maxwell, Physica C **350**, 24 (2001).